

# 418 $\text{cm}^{-1}$ Raman scattering from gallium nitride nanowires: Is it a vibration mode of N-rich Ga–N bond configuration?

J. Q. Ning and S. J. Xu<sup>a)</sup>

*Department of Physics, The University of Hong Kong, Pokfulam Road, Hong Kong, China*

D. P. Yu

*Electron Microscopy Laboratory, School of Physics, Peking University, Beijing 100871, China and State Key Laboratory for Artificial Microstructures and Mesoscopic Physics, School of Physics, Peking University, Beijing 100871, China*

Y. Y. Shan and S. T. Lee

*Department of Physics and Materials Science, City University of Hong Kong, Kowloon, Hong Kong, China*

(Received 15 May 2007; accepted 15 August 2007; published online 6 September 2007)

A Raman-active vibration mode at  $418 \text{ cm}^{-1}$  is observed in wurtzite gallium nitride (GaN) nanowires synthesized by different growth methods. In particular, Raman scattering measurements of a number of GaN nanowires systematically prepared by nitriding  $\beta\text{-Ga}_2\text{O}_3$  nanowires at different temperatures show an interesting evolution of the mode, revealing that it is most likely the vibration mode of N-rich octahedral Ga–N<sub>6</sub> bonds. This idea is further supported by the high-resolution transmission electron microscopic observation. © 2007 American Institute of Physics.

[DOI: 10.1063/1.2780081]

In the past decade, the GaN-based optoelectronic industry has grown rapidly. More recently, various forms of GaN nanomaterials such as nanorods and nanowires have attracted a great deal of attention as these nanosized GaN materials are expected to exhibit superior optical and electrical properties that may greatly extend applications of GaN-based materials. For example, GaN nanorods and nanowires have been used to fabricate light-emitting diodes<sup>1</sup> and field-effect transistors.<sup>2</sup> Further exploitation of devices based on GaN nanomaterials demands a better understanding of the properties of such nanomaterials. Raman scattering is a powerful tool to characterize the structural, compositional, and lattice vibrational properties of a material. The application of this powerful technique to GaN nanomaterials has led to a recent observation of a  $418 \text{ cm}^{-1}$  vibration mode.<sup>3–5</sup> In fact, a careful literature search shows that this Raman peak had been reported earlier in significantly disordered GaN epilayers.<sup>6,7</sup> However, its microstructural origin is still a debated issue. This letter, which is motivated by the noticeable appearance of this Raman mode, shows that it most likely originates from abundant regional N-rich Ga–N bond configurations that exist in various GaN nanostructures and some strongly defected GaN films.

We start our discussion from the typical Raman spectra measured from two kinds of GaN nanostructures synthesized by different methods, as shown in Fig. 1. The Raman spectra were measured at room temperature under the backscattering geometric configuration using WITec-Alpha confocal micro-Raman system. The excitation light was the 514.5 nm line of an Ar<sup>+</sup> laser with 30 mW output power. During the measurements, the excitation light was focused onto the sample surface with a 60× Olympus objective. In Fig. 1, spectrum (a) was recorded from a GaN nanowire sample prepared on a Si substrate by chemical vapor deposition (CVD),<sup>8</sup> while spectrum (b) was from another GaN nanowire sample obtained by nitriding  $\text{Ga}_2\text{O}_3$  nanowires in  $\text{NH}_3$  at  $950^\circ\text{C}$  for 30 min.

In addition to the characteristic Raman peaks at 564 and  $720 \text{ cm}^{-1}$  of wurtzite GaN, one peak at  $418 \text{ cm}^{-1}$  can be well seen in both the spectra. Besides this peak, another additional peak at  $252 \text{ cm}^{-1}$  is observed. Other peaks marked by asterisk are from the Si substrate. It is more interesting to note that spectrum (b) in Fig. 1 exactly resembles the Raman spectrum of the GaN hollow spheres obtained by Sun and Li.<sup>5</sup> These consistent observations of the  $418 \text{ cm}^{-1}$  peak in the GaN nanostructures and in the strongly defected films prepared by different groups with a variety of techniques suggest that the Raman structure is likely to be a characteristic vibration mode of some unknown Ga–N bond configuration which exists abundantly in various forms of nano- and defected GaN structures.

Usually, Raman spectroscopic features of a material can be interpreted in terms of the vibrational density of states (VDOS) which is a measure of the vibrational excitations of the material. The VDOS of GaN has been well studied.<sup>9–11</sup> The structures at 564 and  $720 \text{ cm}^{-1}$  can be readily identified since they just correspond to the TO and LO modes in the VDOS, respectively. However, for the peak at  $418 \text{ cm}^{-1}$ , no corresponding structure exists in the theoretical VDOS of

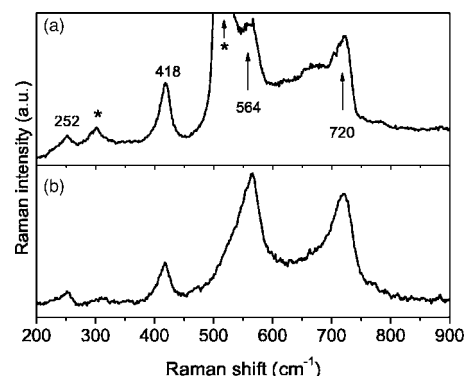


FIG. 1. Room-temperature Raman spectra of the two kinds of GaN nanowires: (a) grown by CVD and (b) obtained by nitriding  $\text{Ga}_2\text{O}_3$  nanowires in  $\text{NH}_3$  at  $950^\circ\text{C}$  for 30 min. The peaks marked by asterisk are from the Si substrate.

<sup>a)</sup> Author to whom correspondence should be addressed; electronic mail: sjxu@hkuc.hku.hk

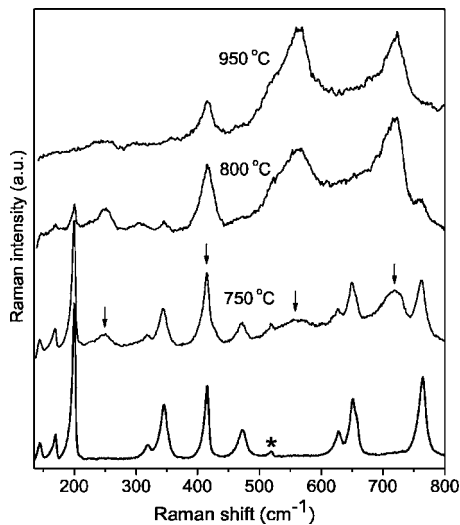


FIG. 2. Raman spectra of  $\text{Ga}_2\text{O}_3$  nanowires nitrided at different temperatures. The fresh Raman peaks indicated by the vertical arrows are due to the formation of GaN compound. The  $520\text{ cm}^{-1}$  peak marked by asterisk in the bottom spectrum is from the substrate Si on which the  $\text{Ga}_2\text{O}_3$  nanowires were grown.

GaN because it lies in the phonon band gap between the acoustic and optical bands of GaN. The peak, therefore, cannot be explained even with disorder-activated Raman scattering and indeed it is not observed in either experimentally measured or theoretically calculated Raman spectra of amorphous GaN.<sup>9,12</sup>

Figure 2 shows the Raman spectra of  $\text{Ga}_2\text{O}_3$  nanowires nitrided at 750, 800, and 950 °C, respectively, under identical ammonia gas flow for 30 min. The typical Raman spectrum of pure  $\beta\text{-Ga}_2\text{O}_3$  nanowires is also plotted for reference. In the reference spectrum, the sharp peaks stem from the different vibrational modes of  $\beta\text{-Ga}_2\text{O}_3$  except for the  $520\text{ cm}^{-1}$  peak of the Si substrate marked by an asterisk. From Fig. 2, one can clearly observe the evolution of the four GaN-related Raman peaks at 252, 418, 564, and  $720\text{ cm}^{-1}$  indicated by vertical arrows. These peaks start to show up in the Raman spectrum of the  $\text{Ga}_2\text{O}_3$  nanowires nitrided at 750 °C and gradually become dominant with increasing nitridation temperature. It is particularly interesting to note that the  $418\text{ cm}^{-1}$  peak evolves from the Raman peak of  $\beta\text{-Ga}_2\text{O}_3$  at  $416\text{ cm}^{-1}$ . This provides an important clue about the microstructural origin of the  $418\text{ cm}^{-1}$  peak.

Figure 3(a) shows a representative high-resolution transmission electron microscopy (HRTEM) image of a  $\text{Ga}_2\text{O}_3$  wire nitrided at 750 °C. The horizontal fringes parallel to the wire axial direction are found to dominate in the image and have a spacing of about  $2.81\text{ \AA}$  which corresponds to the  $d$  spacing of the  $\beta\text{-Ga}_2\text{O}_3$  {002} lattice planes. These facts indicate that the majority of the wire is still  $\beta\text{-Ga}_2\text{O}_3$  although it was nitrided at 750 °C. However, these horizontal fringes do not coherently prolong throughout the entire wire and are broken by many local blurred regions. These regions are believed to be the disordered grains where nitrogen atoms are already incorporated into the lattice of  $\beta\text{-Ga}_2\text{O}_3$ . Such a grain is indicated by a rectangle in Fig. 3(a). Besides the blurred regions, the lattice fringes in some local regions are clearly seen to be tilted at angles of  $60^\circ$  and  $120^\circ$  with respect to the [100] direction. We would like to point out that no corresponding lattice planes of the  $\beta\text{-Ga}_2\text{O}_3$  phase possess such tilting directions or spacing between the tilting

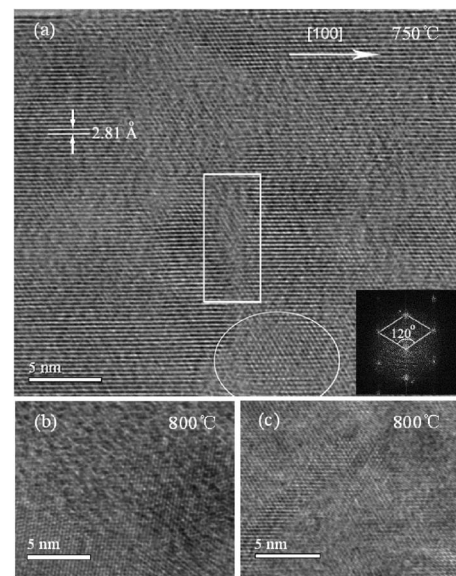


FIG. 3. (a) HRTEM image of a wire treated at 750 °C. The inset is selected-area electron diffraction (SAED) patterns showing hexagonal symmetry. (b) and (c) are the HRTEM images of different wires nitrided at 800 °C, respectively.

fringes. Furthermore, strong distortion of the horizontal fringes can be seen in these regions. For example, in such a region outlined by the elliptical line in Fig. 3(a), the oblique fringes become prominent and the horizontal fringes are significantly distorted. All these structural features can be well interpreted by the incorporation of nitrogen into the local regions. The inset in Fig. 3(a) shows the selected area electron diffraction (SAED) pattern of such a region. Interestingly, the hexagonal diffraction pattern can be seen although it is dimmed by the strong disorders in the region. It can be viewed as further supporting evidence of nitrogen incorporation into local  $\text{Ga}_2\text{O}_3$  lattice regions. We thus conclude that the 750 °C nitridation in our case has led to the N incorporation and formation of local Ga–N bonds inside  $\beta\text{-Ga}_2\text{O}_3$  lattice. Increasingly blurred regions with irregularly oriented fringes are thus expected in HRTEM images of the  $\text{Ga}_2\text{O}_3$  nanowires nitrided at higher temperatures. Indeed, such expectation is verified in the two HRTEM images of the  $\text{Ga}_2\text{O}_3$  nanowires nitrided at 800 °C, as shown in Figs. 3(b) and 3(c). This concurs with the observation of N incorporation made by one of us using x-ray photoelectron spectroscopy and photoluminescence measurements.<sup>13</sup> In the local inclusions embedded into  $\beta\text{-Ga}_2\text{O}_3$ , the Ga–N bond configuration may be significantly different from the normal configuration in the GaN wurtzite phase. Two kinds of Ga–N bond configurations are postulated: one is GaN-like and the other  $\text{Ga}_2\text{O}_3$ -like. GaN-like bonds exhibit vibrational properties which can be interpreted using the VDOS of GaN. For  $\text{Ga}_2\text{O}_3$ -like Ga–N bonds, however, different vibrational properties such as the observed  $418$  and  $252\text{ cm}^{-1}$  peaks are to be expected. It is known that the wurtzite-GaN lattice can be referred to as an arrangement of corner-sharing Ga– $\text{N}_4$  tetrahedra, whereas  $\beta\text{-Ga}_2\text{O}_3$  consists of mixed edge-sharing Ga– $\text{O}_6$  octahedra and corner-sharing Ga– $\text{O}_4$  tetrahedra.<sup>14</sup> The unique mixed bond configurations of  $\beta\text{-Ga}_2\text{O}_3$  crystal thus give rise to more vibration modes than the pure wurtzite phase, as shown in the bottom Raman spectrum in Fig. 2. For instance, the  $416\text{ cm}^{-1}$  peak is an intrinsic vibration mode exactly associated with the Ga– $\text{O}_6$  octahedra in the  $\beta\text{-Ga}_2\text{O}_3$

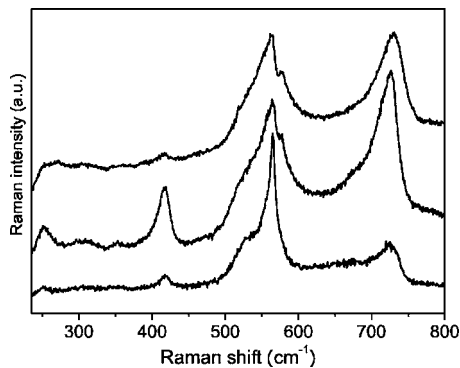


FIG. 4. Raman spectra measured from  $\text{Ga}_2\text{O}_3$  nanowires nitrided in  $\text{NH}_3$  under different conditions: the top at  $1100^\circ\text{C}$  for 20 min, the middle at  $1100^\circ\text{C}$  for 30 min, and the bottom at  $1150^\circ\text{C}$  for 20 min.

lattice.<sup>15</sup> During the nitridation of  $\beta\text{-Ga}_2\text{O}_3$  nanowires, N atoms are expected to replace O atoms either in  $\text{Ga-O}_6$  or in  $\text{Ga-O}_4$  bond configurations. The latter replacement will result in the formation of normal  $\text{Ga-N}_4$  bonds while the former may lead to the formation of local  $\text{Ga-N}_6$  octahedral structures. Of course, it should be pointed out that local  $\text{Ga-N}_x$  structures with  $6 \geq x > 4$  might exist due to incomplete replacement chemical reaction during the nitridation process. These resultant N-rich local structures should bring about some fresh peaks in the Raman spectrum. As shown in Fig. 2, the close relationship between the  $418\text{ cm}^{-1}$  peak of the GaN nanowires and the  $416\text{ cm}^{-1}$  peak from the  $\text{Ga-O}_6$  octahedral structure of  $\beta\text{-Ga}_2\text{O}_3$  gives strong support for the existence of local  $\text{Ga-N}_6$  octahedral structures. As the nitridation temperature is increased, more  $\text{Ga-O}_6$  octahedral structures transform into the  $\text{Ga-N}_6$  bond structures, resulting in an increase of the  $418\text{ cm}^{-1}$  peak in the Raman spectrum, as observed in Fig. 2. However, when the nitridation temperature is high enough, unstable  $\text{Ga-N}_6$  bonds will change into stable  $\text{Ga-N}_4$  bonds. This accounts for the reduction of  $418\text{ cm}^{-1}$  Raman peak intensity from the samples nitrided at  $950^\circ\text{C}$  and above. Such an argument is supported by additional experimental spectra as presented below.

Figure 4 depicts three Raman spectra of  $\text{Ga}_2\text{O}_3$  nanowires nitrided at higher temperatures. The top and middle ones are the Raman spectra from the samples nitrided in ammonia at  $1100^\circ\text{C}$  for 20 and 30 min, respectively, while the bottom is from a sample nitrided at  $1150^\circ\text{C}$  for 20 min. The Raman signals from  $\text{Ga}_2\text{O}_3$  components are no longer observed in these spectra, indicating that almost complete nitridation of  $\text{Ga}_2\text{O}_3$  has occurred under these conditions. In comparison with the top and bottom spectra, the  $418\text{ cm}^{-1}$  peak for the middle spectrum that corresponds to the longer nitridation time is greatly enhanced. This implies that increasing nitridation time favors the formation of the unstable  $\text{Ga-N}_6$  bonds giving the  $418\text{ cm}^{-1}$  peak. However, higher treatment temperature results in the transformation of the unstable  $\text{Ga-N}_6$  bond structure to the stable  $\text{Ga-N}_4$  phase, as indicated by the bottom spectrum in Fig. 4. Here, the peak at  $565\text{ cm}^{-1}$ , which corresponds to the  $E_2$  (high) mode of hexagonal crystalline ZnO, becomes sharper and more dominant, indicating a higher quality hexagonal phase of ZnO.<sup>4,16</sup>

From the discussions given above and the structural nature of octahedral structure, the formation of  $\text{Ga-N}_6$  bond structures requires two conditions, namely, a nitrogen rich condition and a local loosened lattice environment. In fact, all the GaN nanostructures reported in the literature showing the  $418\text{ cm}^{-1}$  Raman peak were obtained in  $\text{N}_2$  or  $\text{NH}_3$  am-

biance providing an excellent N-rich environment.<sup>3-5,8,17</sup> Even in the case of ion-implanted GaN,<sup>18</sup> the N-rich local defected structures with the loosened lattice spacing were formed as Ga atoms are more easily displaced than N atoms. In our case, the original  $\beta\text{-Ga}_2\text{O}_3$  lattice provides an ideal environment for the formation of local  $\text{Ga-N}_6$  octahedral structures during the nitridation due to the existence of  $\text{Ga-O}_6$  octahedra, thus explaining the remarkable vibration mode at  $418\text{ cm}^{-1}$  in the GaN nanowires as obtained by nitriding  $\beta\text{-Ga}_2\text{O}_3$  nanowires. It is worth mentioning that a reversed phase transition of GaN from tetrahedrally bonded structure to an octahedrally bonded structure under high pressure has been realized.<sup>19,20</sup> We also note that in an earlier theoretical work done by Sun *et al.*,<sup>21</sup> it was pointed out that “nonbonding” lone pairs exist on the nitride surface and can lower the Raman frequencies of vibration modes. The experimental results presented in the present study seem consistent with their theoretical prediction although there is no quantitative estimation of the Raman frequency shifts available.

In conclusion, we have shown that the vibrational mode at  $418\text{ cm}^{-1}$  frequently observed in GaN nanostructures most likely originates from octahedrally bonded GaN structures. This conclusion is strongly supported by the observed evolution of the  $418\text{ cm}^{-1}$  mode under postnitridation conditions of  $\beta\text{-Ga}_2\text{O}_3$  nanowires grown on Si substrates.

The authors wish to thank X. M. Cai, A. B. Djurišić, and M. H. Xie for supplying one kind of GaN nanowires grown with CVD. The authors also gratefully thank C. D. Beling for his critical reading of this letter. This work was partially supported by the University Development Fund and the Faculty Development Fund of the University of Hong Kong.

<sup>1</sup>H. M. Kim, Y. H. Choo, H. Lee, S. I. Kim, S. R. Ryu, D. Y. Kim, T. W. Kang, and K. S. Chung, *Nano Lett.* **4**, 1059 (2004).

<sup>2</sup>Y. Huang, X. Duan, Y. Cui, and C. M. Lieber, *Nano Lett.* **2**, 101 (2002).

<sup>3</sup>J. L. Coffey, T. W. Zerda, R. Appel, R. L. Wells, and J. F. Janik, *Chem. Mater.* **11**, 20 (1999).

<sup>4</sup>H. D. Li, S. L. Zhang, H. B. Yang, G. T. Zou, Y. Y. Yang, K. T. Yue, X. H. Wu, and Y. Yan, *J. Appl. Phys.* **91**, 4562 (2002).

<sup>5</sup>Xiaoming Sun and Yadong Li, *Angew. Chem.* **116**, 3915 (2004).

<sup>6</sup>H. Siegle, G. Kaczmarczyk, L. Filippidis, A. P. Litvinchuk, A. Hoffmann, and C. Thomsen, *Phys. Rev. B* **55**, 7000 (1997).

<sup>7</sup>V. Yu. Davydov, Yu. E. Kitaev, I. N. Goncharuk, A. N. Smirnov, J. Graul, O. Semchinova, D. Uffmann, M. B. Smirnov, A. P. Mirgorodsky, and R. A. Evarestov, *Phys. Rev. B* **58**, 12899 (1998).

<sup>8</sup>X. M. Cai, A. B. Djurišić, and M. H. Xie, *Thin Solid Films* **515**, 984 (2006).

<sup>9</sup>W. Pollard, *J. Non-Cryst. Solids* **283**, 203 (2001).

<sup>10</sup>K. Parlinski and Y. Kawazoe, *Phys. Rev. B* **60**, 15511 (1999).

<sup>11</sup>G. Kaczmarczyk, A. Kaschner, A. Hoffmann, and C. Thomsen, *Phys. Rev. B* **61**, 5353 (2000).

<sup>12</sup>H. J. Trodahl, F. Budde, B. J. Ruck, S. Granville, A. Koo, and A. Bittar, *J. Appl. Phys.* **97**, 084309 (2005).

<sup>13</sup>Y. P. Song, H. Z. Zhang, C. Lin, Y. W. Zhu, G. H. Li, F. H. Yang, and D. P. Yu, *Phys. Rev. B* **69**, 075304 (2004).

<sup>14</sup>S. Geller, *J. Chem. Phys.* **33**, 676 (1960).

<sup>15</sup>D. Dohy, G. Lucazeau, and A. Revcolevschi, *J. Solid State Chem.* **45**, 180 (1982).

<sup>16</sup>D. G. Zhao, S. J. Xu, M. H. Xie, S. Y. Tong, and H. Yang, *Appl. Phys. Lett.* **83**, 677 (2003).

<sup>17</sup>C. Vinegoni, M. Cazzanelli, A. Trivelli, G. Mariotto, J. Castro, J. G. Lunney, and J. Levy, *Surf. Coat. Technol.* **124**, 272 (2000).

<sup>18</sup>W. Limmer, W. Ritter, and R. Sauer, *Appl. Phys. Lett.* **72**, 2589 (1998).

<sup>19</sup>M. Ueno, M. Yoshida, A. Onodera, O. Shimomura, and K. Takemura, *AIP Conf. Proc.* **309**, 557 (1994).

<sup>20</sup>S. Limpitjumnong and W. R. L. Lambrecht, *Phys. Rev. Lett.* **86**, 91 (2001).

<sup>21</sup>C. Q. Sun, B. K. Tay, S. P. Lau, X. W. Sun, X. T. Zeng, S. Liu, H. L. Bai, H. Liu, Z. H. Liu, and E. Y. Jiang, *J. Appl. Phys.* **90**, 2615 (2001).